Progress In Electromagnetics Research Letters, Vol. 54, 79–84, 2015

Analytical Solution for Capacitance and Characteristic Impedance of CPW with Defected Structures in Signal line

Naibo Zhang[1], Zhongliang Deng[2], Lingmin Shao[1], and Jun Yang[1, *]

Abstract—This paper presents an analytical solution for capacitance and characteristic impedance of CPW with defected structures (CPW_DS) in signal line. The first category of incomplete elliptic integrals $F(\phi, k)$ is employed for calculation, and the capacitance and characteristic impedance of CPW_GS in signal line are first time achieved by the analytical solution. FEM simulation results are used to verify the results of analytical solution, which shows a good agreement. All calculations are completed in software *Wolfram Mathematica*, and CPW structures are simulated in software *HFSS*.

1. INTRODUCTION

Coplanar waveguide (CPW) has found a wide range of applications in the design of uniplanar monolithic microwave integrated circuits (MMICs) including multilayered geometry because of its attractive features such as low-frequency dispersion, easy insertion of shunt and series active devices, and less substrate dependence [1, 2]. The CPW has been widely studied. For example, characteristic impedance, capacitance and equivalent circuits, and many methods are used to study CPW [3–12]. However, most papers discuss regular CPW structures, and few repots are about CPW with defected structures (CPW_DS). CPW_DS is widely used in RF devices [12], such as filter [13, 14], antenna [15], and phase shifter. The defected structure in CPW can largely affect CPW capacitance, impedance and equivalent circuit [2]. Zhu and Wu [2] presented a method of a parametric-extraction (short-open calibration) developed from field results and used for equivalent-circuit modeling, but the "Full-Wave MoM Algorithm" and SOC analysis in the paper cannot well solve the characteristics of CPW_DS. Linner and Kollberg [6] presented CAD models for shielded multilayered CPW. All CPW structures in this paper are regular, and the method used in the paper is conformal mapping; however, the first category of complete elliptic integrals $K(k)$ and the solution in this paper cannot obtain the capacitance and impedance of CPW_GS.

In this paper, conformal mapping method is also employed for capacitance and characteristic impedance of CPW_GS. Although the conformal mapping is a familiar method, the different points in this paper are: 1) Import the first category of incomplete elliptic integrals $F(\phi, k)$ to obtain capacitance and characteristic impedance of CPW_GS. 2) First time to obtain the analytical solution for capacitance and characteristic impedance of CPW_GS. FEM simulation results are used to verify the analytical solution, and the numerical results show that analytical solution in this paper is a good way to calculate the capacitance and characteristic impedance of CPW_DS in signal line.

2. ANALYZE CAPACITANCE AND CHARACTERISTIC IMPEDANCE OF CPW_GS IN SIGNAL LINE

The capacitance and characteristic impedance of CPW_DS in signal line are analyzed by dividing into air layer and dielectric layer. The finite height and width of ground are analyzed in this paper, and

Received 12 May 2015, Accepted 14 July 2015, Scheduled 22 July 2015

* Corresponding author: Jun Yang (jyang@eng.uwo.ca).

[1] Department of Mechanical and Materials Engineering, The University of Western Ontario, London, Canada. [2] School of Electronic Engineering, Beijing University of Posts and Telecommunications, Beijing 100876, China.

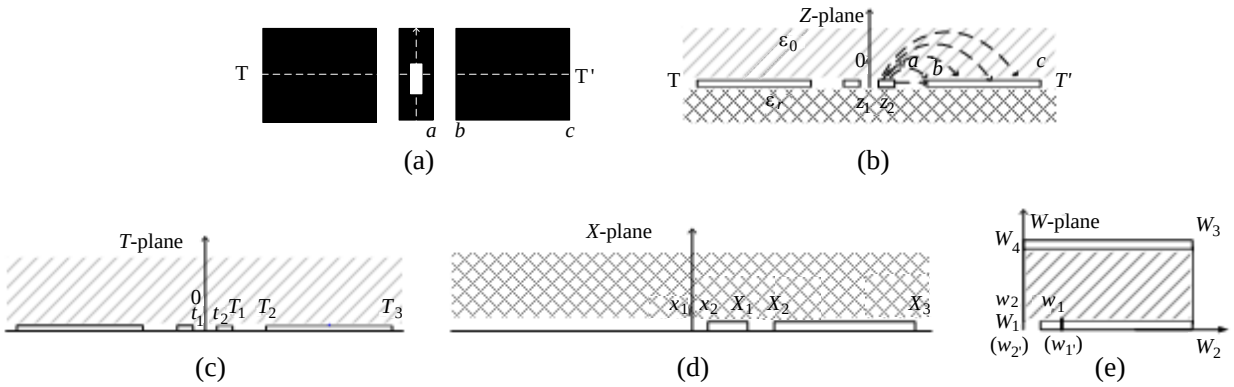

Figure 1. (a) The CPW structure with DS in signal line; (b) the side view of CPW structure; (c) map to T-plane; (d) map to X-plane; (e) map to W-plane (parallel capacitor) [1].

the thickness of metal layer is ignored. Figure 1(a) shows a CPW_DS in the middle of signal line with characteristic impedance of Z_0, and the characteristic impedance with no DS is $50\,\Omega$. Figure 1(b) is a side view of Figure 1(a), in which the top layer is air (ε_0), and bottom layer is dielectric substrate ($\varepsilon_r\varepsilon_0$). Figures 1(c)–(d) correspond to T-plane and X-plane mappings from Figure 1(b), respectively. Figure 1(e) is W-plane mappings from Figure 1(c) and Figure 1(d). The T-plane is transferred from Z-plane by function $t = z^3$ [12]. The coordinates in T-plane, t_1, t_2, T_1, T_2 and T_3 correspond to the coordinates in Z-plane z_1, z_2, a, b and c. After transformation, T-plane is only a positive plane. The dielectric layer is transferred to X-plane through the function $x = \cosh^2(\pi z/2h)$ [16]. The zero point in Z-plane corresponds to 1 in the X-plane, and the rests correspond to x_2, X_1, X_2, and X_3. The zero point in T-plane is transformed to W_1 in the W-plane, and the other coordinates t_1, t_2, T_1, T_2 and T_3 correspond to w_1, w_2, W_2, W_3 and W_4 in W-plane, respectively. The x_1, x_2, X_1, X_2, and X_3 correspond to w_1', w_2', W_2, W_3 and W_4 in W-plane as well.

2.1. Air Layer Analysis

The air layer in Figure 1(c) is analyzed by using conformal mapping method. The capacitance and characteristic impedance of CPW_DS in signal line are obtained by analyzing Schwarz transformation, $K(k)$ and $F(\varphi, k)$. From Schwarz polygon transformation [16], the relationship between T- and W-planes is expressed as,

$$\frac{dw}{dt} = A \prod_{i=1}^{n} (t - t_i)^{\frac{\alpha_i}{\pi} - 1} \tag{1}$$

When T-plane maps to W-plane, the coordinates $-T_1$, $-T_2$, $-t_1$, $-t_2$, T_1, T_2, t_1, t_2 correspond to angles of $pi/2$, $pi/2$, pi, pi, $pi/2$, $pi/2$, pi, and pi, respectively, then, $w = A\int_0^{T_1} \frac{dt}{\sqrt{(t^2-T_1^2)(t^2-T_2^2)}}$, the parameter are defined as $t' = \frac{t}{T_1}$, $k = \frac{T_1}{T_2}$. And then, the relationship between T- and W-planes is expressed as,

$$w = Ak \int_0^1 \frac{dt'}{\sqrt{(1-t'^2)\,(1-k^2t'^2)}} \tag{2}$$

According to boundary condition [9, 16], where Ak equals 1, and then w equals the first category of complete elliptic integrals $K(k)$. The air layer capacitance with no defected structure is expressed as,

$$C_a = 4\varepsilon_0 \frac{K(k_1)}{K(k_1')}, \quad k_1 = k = \frac{T_1}{T_2}, \quad k_1' = \sqrt{1-k_1^2}\ [16] \tag{3}$$

where C_a is the capacitance with no defected structure in CPW signal line; k_1 and k_1' are the coefficients; ε_0 is the permittivity of vacuum. The air layer capacitance with defected structure is expressed as,

$$C_{air} = C_a - C_{ads} \tag{4}$$

where C_{air} is the capacitance with defected structure in CPW signal line and C_{ads} the capacitance of defected structure (slot) in CPW signal. The thickness of metal layer is ignored, and the capacitance is expressed as,

$$C_{ads} = 4\varepsilon_0 \frac{\overline{w_1 w_2}}{\overline{W_2 W_3}} \tag{5}$$

where, $\overline{W_2 W_3} = K(k_1')$ and $\overline{w_1 w_2} = w_2 - w_1$. The coordinate points w_2 and w_1 are expressed as following,

$$w_2 = A\int_0^{t_2} \frac{dt}{\sqrt{(t^2 - T_1^2)(t^2 - T_2^2)}} = \int_0^{t_2/T_1} \frac{dt'}{\sqrt{(1-t'^2)(1-k^2t'^2)}} = F[\arcsin(t_2/T_1), k_1] \tag{6}$$

$$w_1 = \int_0^{t_1/T_1} \frac{dt'}{\sqrt{(1-t'^2)(1-k^2t'^2)}} = F[\arcsin(t_1/T_1), k_1] \tag{7}$$

Equations (6) and (7) are the first category of incomplete elliptic integrals, and then,

$$\overline{w_1 w_2} = F[\arcsin(t_2/T_1), k_1] - F[\arcsin(t_1/T_1), k_1] \tag{8}$$

where $F[\arcsin(t_2/T_1), k]$ and $F[\arcsin(t_1/T_1), k]$ are the first category of incomplete elliptic integrals. According to Equations (3)–(5), (8), the capacitance of air layer is expressed as following,

$$C_{air} = 4\varepsilon_0 \frac{K(k_1) + F[\arcsin(t_1/T_1), k_1] - F[\arcsin(t_2/T_1), k_1]}{K(k_1')} \tag{9}$$

2.2. Dielectric Layer Analysis

The analysis steps of dielectric layer in Figure 1(d) is the same as air layer, and the detailed analyzing process is ignored. The capacitance results are expressed as following,

$$C_e = 2\varepsilon_0(\varepsilon_r - 1)\frac{K(k_2)}{K(k_2')} \text{ [9]} \tag{10}$$

where C_e is the capacitance of dielectric layer and ε_r the permittivity of substrate. The coefficients k_2, k_2' are expressed as,

$$k_2 = \frac{\sinh(\pi a/4h)}{\sinh(\pi b/4h)} \quad k_2' = \sqrt{1-k_2^2} \text{ [9]} \tag{11}$$

where h is the height of substrate.

The capacitance of CPW with defected structure in middle signal line is expressed as,

$$C_1 = C_e - C_{eds} = 2\varepsilon_0(\varepsilon_r - 1)\frac{K(k_2) + F[\arcsin(x_1/X_1), k_3] - F[\arcsin(x_2/X_1), k_3]}{K(k_2')}$$

$$k_3 = \frac{X_1}{X_2} = \frac{\cosh^2\left(\dfrac{\pi a}{2h}\right)}{\cosh^2\left(\dfrac{\pi b}{2h}\right)} \tag{12}$$

where C_1 is capacitance of CPW with defected structure in middle signal line and C_{eds} the capacitance of defected structure in CPW signal.

Therefore, the total capacitance can be represented as the sum of capacitance C_{air} corresponding to the air layer and capacitance C_1 corresponding to the dielectric layer, which can be expressed as,

$$C_{cpw} = C_1 + C_{air} = 2\varepsilon_0 \left\{ \begin{array}{l} 2\dfrac{K(k_1) + F[\arcsin(t_1/T_1), k_1] - F[\arcsin(t_2/T_1), k_1]}{K(k_1')} \\ +(\varepsilon_r - 1)\dfrac{K(k_2) + F[\arcsin(x_1/X_1), k_3] - F[\arcsin(x_2/X_1), k_3]}{K(k_2')} \end{array} \right\} \tag{13}$$

According to [8], the characteristic impedance of the structure is as follows,

$$Z_{0c} = \frac{1}{c\sqrt{C_{cpw}C_{air}}} \tag{14}$$

3. NUMERICAL RESULTS

The defected structure is shown in Figure 2(a). The dimensions are marked in the figure with only one variable parameter L changing from 4 mm to 15.6 mm. The substrate is FR-4 with permittivity of 4.8, thickness of 1.6 mm and tangent angle loss of 0.017. Figure 2(b) is the equivalent circuit of Figure 2(a), which is used to calculate the characteristic impedance of CPW with defected structure and compare with the results from Equation (14). The method is 1) simulate the structure by HFSS (FEM simulation) and get the input impedance from Smith Chart, 2) obtain the characteristic impedance through input impedance formula, and then, compared with the results of Equations (14). The detailed process is as following. The characteristic impedance Z_{0s} in Figure 2(a) is (Z_l is 50 Ω),

$$Z_{0s} = \frac{Z_{in} - 50 + \sqrt{Z_{in}^2 + 2500 - 100Z_{in} - 200Z_{in}\tan^2\theta}}{2j\tan\theta} \tag{15}$$

where $\theta = \frac{2\pi l}{\lambda}$, l equals 50 cm, and then $\theta = \frac{9\pi}{4}$ @ 0.675 GHz.

The characteristic impedance Z_{0s} is obtained by simulating CPW structures and calculating Equation (15). The details are shown in Table 1. According to the dimensions in Figure 2(a), the coefficients k_1, k_1', k_2 and k_2' are 0.703, 0.711, 0.612 and 0.79, respectively. The capacitances C_{air}, C_1, C_{cpw} and characteristic impedance Z_{0c} are calculated by Equations (9) and (12)–(14). The data are shown in Table 1.

Figures 3(a)–(c) show the relationship among capacitances C_1, C_{air}, C_{cpw} and CPW structure L. When L changes from 0 mm to 13 mm, the capacitance C_1 keeps almost constant and changes quickly from 13 mm to 15.6 mm. When L changes from 4 mm to 13 mm, the capacitance C_{cpw} altered by 12.6 pF, but when the dimension L changes from 13 mm to 15.6 mm, the capacitance altered by 72.03 pF, which

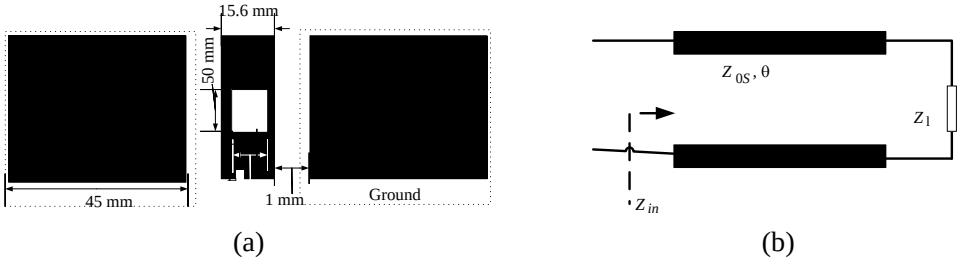

Figure 2. (a) The simulation structure based on substrate FR-4 with permittivity of 4.8, thickness of 1.6 mm and tangent angle loss of 0.017, (b) the equivalent circuit of Figure 2(a).

Table 1. Data of capacitance and characteristic impedance corresponding to dimension L.

L (mm)	C_1 (pF)	C_{air} (pF)	C_{cpw} (pF)	Z_{0c} (ohm)	Z_{0s} (Ω) ($\approx$)
15.6	9.93	0	9.93	∞	∞
15	40.56	13.72	54.28	122.14	121.1
14.4	49.47	18.32	67.79	94.59	93.5
14	52.66	20.62	73.28	85.75	84.73
13.6	54.69	22.21	76.9	80.65	78.79
13	56.64	24.69	81.33	73.98	72.1
12	58.14	27.26	85.4	69.09	67.4
10	58.85	30.8	89.65	63.44	61.8
8	58.94	33.01	91.95	60.5	59.4
4	58.94	34.96	93.9	58.18	57.5

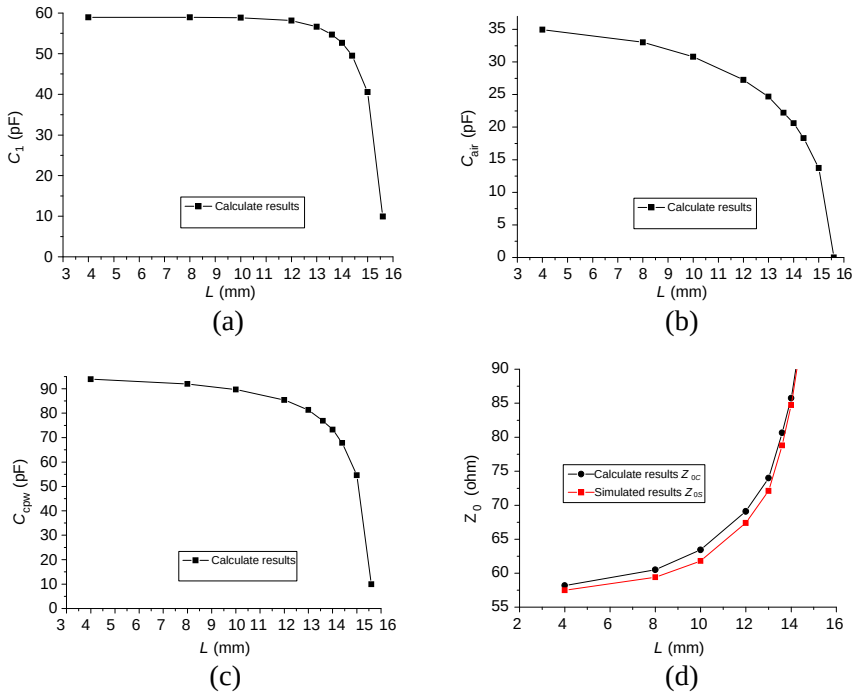

Figure 3. (a) The capacitance C_1, (b) the capacitance C_{air}, (c) the capacitance C_{cpw}, (d) the calculated Z_{0c} and simulated Z_{0s}.

means that the CPW capacitance changes almost 14.98% (12.6/84.1) when CPW structure L changes 83.3% (13/15.6), and the capacitance changes 85.02% when L changes the last 16.7%. The capacitance C_{air} changes much slower than capacitance C_1 and C_{cpw}.

Figure 3(d) shows the calculated Z_{0c} and simulated Z_{0s}. The results show a good agreement between Z_{0c} and Z_{0s}, which means that the analytical solution for capacitance and characteristic impedance is effective. However, there is a little difference between them because of some errors in calculation and simulation.

4. CONCLUSION

In this paper, CPW_DS in signal line is analyzed. The capacitance and characteristic impedance of CPW_DS are obtained by conformal mapping. The Schwartz-Christoffel transformation and the first category of complete/incomplete elliptic integrals $K(k)$, $F(\phi, k)$ are used for obtaining the coordinates of slot in signal line. The capacitance of CPW is achieved by air layer and dielectric layer. The numerical results of CPW with defected structure are analyzed and show that analytical solution is a good way to calculate the capacitance and characteristic impedance.

ACKNOWLEDGMENT

The authors are grateful for financial support from the Natural Science and Engineering Research Council of Canada (NSERC), Canada Foundation for Innovation (CFI) and Research Accelerator Grant of The University of Western Ontario.

REFERENCES

1. Gupta, K. C., R. Garg, I. Bahl, and P. Bhartia, "Coplanar lines: Coplanar waveguide and coplanar strips," *Microstrip Lines and Slot lines*, 2nd Edition, Chapter 7, Artech House, Norwood, MA, 1996.

2. Zhu, L. and K. Wu, "Characterization of finite-ground CPW reactive series-connected elements for innovative design of uniplanar M(H)MICs" *IEEE Trans. Microw. Theory Tech.*, Vol. 50, No. 2, 549–557, Feb. 2002.
3. Wen, C. P., "Coplanar waveguide: A Surface strip transmission line suitable for non-reciprocal gyromagnetic device application," *IEEE Trans. Microw. Theory Tech.*, Vol. 18, No. 17, 1087–1090, 1969.
4. Davis, M. E., et al., "Finite boundary corrections to the coplanar waveguide analysis," *IEEE Trans. Microw. Theory Tech.*, Vol. 21, No. 9, 594–596, 1973.
5. Dib, N. I., M. Gupta, G. E. Ponchak, and L. P. B. Katehi, "Characterization of asymmetric coplanar waveguide discontinuities," *IEEE Trans. Microw. Theory Tech.*, Vol. 41, No. 9, 345–352, Sep. 1993.
6. Linner, L. J. P. and E. L. Kollberg, "CAD models for shielded multilayered CPW," *IEEE Trans. Microw. Theory Tech.*, Vol. 43, No. 4, 772–779, Apr. 1995.
7. Zhu, L., "Unified 3-D definition of CPW- and CSL-mode characteristic impedances of coplanar waveguide using MOM-SOC technique," *IEEE Microwave and Wireless Components Letters*, Vol. 13, No. 4, 158–160, 2003.
8. Dib, N., "Comprehensive study of CAD models of several coplanar waveguide (CPW) discontinuities," *IEE Proc. Microw. Antennas Propag.*, Vol. 152, No. 2, 69–76, Apr. 2005.
9. Simons, R., *Coplanar Waveguide Circuits, Components, and System*, John Wiley & Sons, Ann Arbor, 2001.
10. Zhang, X. and T. Miyoshi, "Optimum design of coplanar waveguide for $LiNbO_3$ optical modulator," *IEEE Trans. Microw. Theory Tech.*, Vol. 43, No. 3, 523–528, 1995.
11. Davis, M. E., et al., "Finite boundary corrections to the coplanar waveguide analysis," *IEEE Trans. Microw. Theory Tech.*, Vol. 21, No. 9, 594–596, 1973.
12. Fang, S., "Study on the characteristic and field pattern of asymmetric coplanar waveguides," Doctoral Thesis, Dalian Maritime University, Feb. 2001.
13. Zhang, N.-B. and Z.-L. Deng, "Method to design microwave band-stop filter based on CPW," *Electronics Letters*, Vol. 47, No. 8, 450–451, Mar. 2011.
14. Guo, X. L., C. Xu, G. A. Zhang, Z. J. Zhang, H. H. Yin, and Z. L. Wang, "Tunable low-pass MEMS filter using defected ground structures (DGS)," *Solid-State Electronics*, Vol. 94, No. 6, 28–31, 2014.
15. Zhang, C., J. Zhang, and L. Li, "Triple band-notched UWB antenna based on SIR-DGS and fork-shaped stubs," *Electronics Letters*, Vol. 50, No. 2, 67–69, Jan. 2013.
16. Liang, C., *Concise Microwave*, 163–164, Higher Education Press, 2006.